Lagrangian path integrals and fluctuations in random flow

Boris I. Shraiman
AT&T Bell Laboratories, 600 Mountain Avenue, Murray Hill, New Jersey 07974

Eric D. Siggia
Laboratory of Atomic and Solid State Physics, Cornell University, Ithaca, New York 14853-2501
(Received 23 June 1993)

The problem of the asymptotic behavior of the probability distribution function (PDF) of a scalar field advected by Gaussian random flow is investigated using the Lagrangian path-integral approach, which naturally captures the physics of transport and dissipation relevant to the problem. For a single-scale random-velocity field and in the presence of a mean scalar gradient we find that the one-point PDF's of both the scalar and its gradient have exponential tails. Under the same conditions the normalized gradient skewness scales with Peclet number to approximately -0.3 power.

PACS number(s): 47.27.−i, 05.40.+j

I. INTRODUCTION

The fluctuations in turbulent flows are most naturally quantified by a probability distribution function (PDF) which is directly measurable experimentally [1–6]. The PDF at a given point is constructed as a histogram of the time series of the fluctuating field. The interesting single-point measurements involve velocity, pressure, or advected scalar, either passive (e.g., a dye) or active (e.g., the temperature in convection). With a pair of probes or in the presence of a mean flow, from pairs of temporal recordings one can construct PDF's of relative velocities or temperature differences for points separated by a distance r and, in the limit of $r\rightarrow 0$, the derivatives. The experimental measurements of the PDF of velocity differences (as well as temperature gradients) were reported by Van Atta and Park [1], Anselmet *et al.* [2], and Castaing, Gagne, and Hopfinger [3] for a variety of wind tunnel flows. The PDF's of temperature fluctuations have been studied by Castaing *et al.* [4] for turbulent Rayleigh-Benard convection, and by Gollub *et al.* [5], Jayesh and Warhaft [6], and Thoroddsen and Van Atta [7] for externally forced flows. While the PDF of the velocity at a point (in a reasonably isotropic turbulent flow) is Gaussian, the PDF's of other quantities are typically *not* Gaussian and exhibit characteristic *long tails.*

In particular, the PDF's of velocity differences for inertial range separations are markedly non-Gaussian and rather appear to fall off exponentially [1–3]. Asymptotically exponential PDF's of local temperature are observed in turbulent Rayleigh-Benard convection and in forced turbulent flow with a large-scale temperature gradient [4–6]. On the other hand, the PDF's of both velocity and temperature derivatives [1–3] in turbulent flows appear to have considerably slower than exponential, perhaps "stretch" exponential, i.e., $\exp(-x^{\gamma})$, decays.

The large fluctuation statistics of the advected scalar is qualitatively similar in its non-Gaussian nature to that of the velocity differences, which suggests that much can be learned from understanding the relatively simple problem of a passive scalar advected by a synthetic random flow [8–16]. Thus below we shall study the statistics of large fluctuations of a scalar and a scalar gradient in a Gaussian random flow.

In Sec. II we shall formulate the problem of the passive scalar advected by the random incompressible velocity field and specify the conditions under which we can solve for the statistics of the scalar. Since the scalar is passive, the tails of its distribution arise from the rare configurations of the velocity field which bring an element of the fluid from afar to the point of observation, without much mixing and dissipation along the way. Even if the scalar field value for the fluid element was close to the mean at the point of origin, at the observation point it will appear as a large fluctuation. The appropriate theoretical tool for calculating the probability of such velocity configurations is the Lagrangian path integral developed in Sec. III. The scalar PDF is shown to be exponential (for values exceeding the variance) in Sec. IV. The scalar gradient PDF is studied in Sec. V and is shown to be also asymptotically exponential for a single-scale velocity field.

II. THE PASSIVE SCALAR PROBLEM

Let us consider the passive scalar $T(\vec{r})$, advected by a Gaussian random incompressible flow $v_a(\vec{r})$ in d dimensions [8,9]:

$$\partial_t T+\vec{v}\cdot\vec{\nabla}T=\kappa_0\nabla^2 T \ , \tag{2.1}$$

where κ_0 is molecular diffusivity and $\vec{\nabla}\cdot\vec{v}=0$. Assume a single-scale velocity field with characteristic length scale ξ and correlation time τ:

$$\langle v_a(\vec{r},t)v_b(\vec{0},0)\rangle=\Pi_{ab}V^2e^{-|r|/\xi}e^{-|t|/\tau} \ , \tag{2.2}$$

where $\Pi_{ab}(r)$ is a suitable projection operator which makes the divergence on either the a or b index 0. Physically, the correlation time should be roughly the "eddy turnover" time $\tau\sim\xi/V$, but it will be useful to consider the white noise $\tau\ll\xi/V$ and the "frozen" random field

$\tau \gg \xi/V$ limits as well. The ensemble average in (2.2) is over the realizations of the random field.

The scalar field is "forced" by imposing a large-scale gradient $\langle T(\vec{r})\rangle = \vec{g}\cdot\vec{r}$. Let us define the rescaled fluctuating scalar field $\theta(\vec{r}) \equiv [T(\vec{r}) - \vec{g}\cdot\vec{r}]/(|\vec{g}|\xi)$ and nondimensionalize $\vec{r}/\xi \to \vec{r}$, $tV/\xi \to t$. Then, for $\vec{g} = -\hat{\vec{x}}$, we obtain

$$\partial_t \theta + \vec{v}\cdot\vec{\nabla}\theta - \kappa\nabla^2\theta = v_x \ , \tag{2.3}$$

where $\kappa \equiv (V\xi/\kappa_0)^{-1} = \mathrm{Pe}^{-1}$, the inverse of the Peclet number, will be assumed small. (We will occasionally restore the dimensionful symbols V,ξ in what follows, when we want to emphasize units.)

We shall be interested in the probability distribution functions of the scalar at a given point,

$$P(\theta,\vec{r},t) \equiv \langle \delta(\theta - \theta(\vec{r},t)) \rangle \ , \tag{2.4a}$$

and similarly for its gradient,

$$P(\partial_a\theta,\vec{r},t) = \langle \delta(\partial_a\theta - \partial_a\theta(\vec{r},t)) \rangle \ . \tag{2.4b}$$

Since stationary statistics are expected, these PDF's will be time independent and the ensemble average on the right-hand side (RHS) can be replaced by the time average. Further, because of the translational invariance (after averaging), the PDF's do not depend on $\vec{r}$ either. It will be convenient to work with generating functions, e.g.,

$$\hat{P}(\lambda) \equiv \int d\theta\, e^{i\lambda\theta} P(\theta) \ . \tag{2.5}$$

Any distribution function involving the scalar is only meaningful after such times as the advection and diffusion terms have come into balance. Acting alone, say, on initial data $T \propto \vec{g}\cdot\vec{r}$, advection will yield a Gaussian scalar PDF with variance $\sim t$ characteristic of a random walk since T acts as a Lagrangian marker. Pure diffusion will also reduce any distribution to a Gaussian with variance $\sim 1/t$. A very phenomenological model incorporating the balance of advection and diffusion was considered in [15,16] and shown to give exponential tails for θ in (2.3). Evidently, the tails of the scalar PDF arise from improbable events in which a parcel of fluid moves a distance $\gg \xi$ along the mean gradient without equilibrating. More precisely, we show that this occurs because of fluctuations in the shear-assisted mixing rate along a typical path [17] rather than the converse: typical mixing along an atypical jetlike path. In either event the problem reduces to finding the probability of all velocity fields which yield the desired $\delta\theta$ [18] or, in more physical terms, computing the effects of dissipation in a Lagrangian representation.

Another important aspect of physics concerns the distinction between the scalar and the gradient of the scalar. The scalar is conserved, dominated by wave vectors $\sim\xi^{-1}$, and consequently transported by the nearly Gaussian large-scale velocity, with the smaller scales which are present in a real high-Reynolds-number flow acting as an eddy diffusivity. By contrast, the scalar gradient is not conserved and is amplified by the strain, which is a small-scale quantity, very non-Gaussian, and not well characterized in the present state of turbulence theory. While calculating the statistics of the large-scale strain-induced mixing along the Lagrangian trajectory will describe the scalar fluctuations, more is required for the gradient. Experimentally, the distribution of the scalar gradient is profoundly intermittent with relatively large well-mixed regions, where the gradient is minimal, interspersed with sheetlike high gradient structures [3,19,20].

The calculations which follow deal with a *single*-scale random velocity field [i.e., the velocity spectrum is confined to a shell of wave numbers $q \sim \xi^{-1}$, as stated in (2.2)] and small κ_0, for which our approach is most transparent. The Peclet number $\mathrm{Pe} = \kappa^{-1}$ should be large. This could be achieved experimentally by adding a high-molecular-weight dye to randomly stirred fluid at moderate Reynolds numbers. The physics of this single-scale regime corresponds to the Batchelor regime [8–10] which is conventionally realized in high-Reynolds- and high-Prandtl-number flow in the range of scale below the viscous but above the scalar dissipation cutoff. (The k^{-1} spectrum derived by Batchelor [8] arises due to the scalar folding into sheets of variable thickness down to the dissipation scale while keeping the variance of the scalar difference independent of the separation between points to within logs. The experimental consequence is that if the probe does not resolve the thinnest layers, it will average effectively over several realizations of the true single-point scalar distribution, suppressing the non-Gaussian aspects of the latter. This situation is to be contrasted with the case of the Kolmogorov-like, $k^{-5/3}$, scalar spectrum where the local value of θ is dominated by the largest-scale modes and the averaging due to the finite probe size is immaterial.)

Physically, once $\mathrm{Re} > 10^3$, the simplest eddy-diffusion ideas would suggest that the small-scale turbulent fluctuations renormalize κ_0 upwards so that the effective turbulent Peclet number defined for the integral scale of the flow, ξ, is $O(1)$. This would appear to completely vitiate our approximations which require that the mixing is controlled entirely by the large-scale strain rate. In other words, there would not be a significant variation in mixing time with the large-scale strain, and one would expect a Gaussian scalar PDF. This line of reasoning we believe to be oversimplified, because the small-scale velocity modes responsible for the enhanced diffusivity are themselves only present because of the large-scale strain acting in the same $O(\xi)$ region. The simplest dimensional reasoning makes the eddy diffusivity vary linearly with the strain. Therefore, the mixing time varies inversely with the strain rate, as it does (to within an unessential logarithm) for the single-scale velocity field we treat. Once it is accepted that the mixing time is governed by the large-scale strain, the tails of the scalar PDF simply reflect a certain strain history, whose probability can be reasonably calculated within the model we employ. (A more refined treatment of a large Re velocity field is a problem of turbulence, not scalar advection, and beyond our capabilities.) The situation is more complicated for the scalar gradient and all discussion on approximations and applications to experiment are reserved for the Conclusion.

III. THE GREEN'S FUNCTION AND THE SEMICLASSICAL APPROXIMATION

The Lagrangian dynamics is made evident by the Green's-function solution of (2.3):

$$\theta(r',t')=\int_{-\infty}^{t'} dt \int dr\, v_x(r,t)G(r',t'|r,t)\ , \tag{3.1}$$

where the Green's function is defined by the path integral

$$G(r',t'|r,t) \equiv \int_{\substack{r(t)=r\\ r(t')=r'}} \mathrm{D}r\, \exp\left[-\frac{1}{4\kappa}\int_t^{t'} dt''[\dot r_a - v_a(r,t'')]^2\right]\ , \tag{3.2}$$

which solves Eq. (2.3) with the RHS replaced by a δ-function source. In the absence of the flow ($v_a=0$), the RHS of (3.2) becomes the diffusion kernel. In general, however, it is a *functional* of $\vec v(r,t)$ so that $G(r',t'|r,t)>0$ is a random number.

The velocity ensemble-averaged Green's function becomes again a diffusion kernel (for times long compared to τ):

$$\langle G(0,0|r,t)\rangle \sim e^{-r^2/4D|t|}\ , \tag{3.3}$$

with an effective diffusivity (in the limit of small κ_0),

$$D\equiv\int_0^\infty dt\langle v_a(\bar r(t),t)v_a(0,0)\rangle\ , \tag{3.4}$$

given by the Taylor formula [11] involving the velocity correlator along the Lagrangian trajectory $\bar r(t)$ with $r(0)=0$. This expression is true for an arbitrary velocity correlation time τ. In particular, we define the white-noise limit $\tau \ll \xi/V$, as being taken with $D\sim\tau V^2$ fixed.

The behavior of the *unaveraged* propagator can be anticipated on physical grounds, as the subsequent calculation confirms. For $|t|$ less than a velocity-dependent mixing time t_*, $G(0,0|rt)$ is concentrated along the Lagrangian trajectory $\bar r(t)$ defined by $\bar r(0)=0$ and only at $t\approx t_*$ acquires a spread $\sim\xi$, which signals the onset of dissipation. The point where the mixing turns on can be defined as

$$\begin{aligned}\vec r_* \equiv \lim_{t\to\infty}\int dr\,\vec r G(0,0|rt) &= \int_{-\infty}^0 dt\int dr\,\vec v G(0,0|rt)\\ &\simeq \int_{-t_*}^0 dt\,\vec v(\bar r(t),t)\\ &=\bar r(t_*)\ .\end{aligned} \tag{3.5}$$

The second equality expresses an exact property of G, namely, that (2.3) can be solved by initializing (2.1) with $T=x$ and then evolving for a long time. Evidently, from Eq. (3.1) $\theta(0,0)$ is nothing but x_*. The second line in (3.5) recognizes that the t integral is cutoff when G spreads sufficiently in r that the spatial integral over v averages out. This cutoff time by definition is t_*.

Finally, for $|t|\gg t_*$, G explores a volume $\gg\xi^3$ and therefore self-averages, so in conformity with (3.3),

$$G(0,0|r,t)\sim e^{-(\vec r-\vec r_*)^2/4D|t|}\ , \tag{3.6}$$

where the only memory of the earlier history enters via r_* determined by (3.5). Thus the fluctuation effects that determine the tails of $P(\theta)$ are compactly parametrized by t_*, the existence of which motivates the subsequent calculations in this section.

For $|t|<t_*$, G can be calculated in the semiclassical approximation, i.e., in the small-κ limit, where the path integral is dominated by the *classical* trajectories that minimize the action

$$S(t',t)\equiv\tfrac{1}{2}\int_t^{t'} dt''[\dot r_a - v_a(r,t'')]^2\ .$$

This classical dynamics is defined by the Hamiltonian $H(\vec r,\vec p,t)=\frac{1}{2}\vec p^{\,2}+\vec p\cdot\vec v(r,t)$, which is equivalent to the Lagrangian $(\dot r - v)^2/2$. The equations of motion are

$$\dot r_a = v_a + p_a\ , \tag{3.7a}$$

$$\dot p_a = -\partial_a v_b p_b\ . \tag{3.7b}$$

The absolute minimum, $S=0$, is realized for $p_a=0$, $\dot r_a=v_a$, i.e., the unique Lagrangian trajectory passing through a given point. Hence, for a given $v_a(r,t)$, G is concentrated along the Lagrangian trajectory which reaches $r=0$ at $t=0$.

This suggests a linearized approximation for the Green's function which is developed as follows: First, we introduce the momentum variable $\vec p(t)$ as the Legendre transform field in the path integral after shifting the variable of integration $r=\bar r+\eta$ by the Lagrangian trajectory $\bar r(t)$, viz.,

$$\begin{aligned}G(r',0|r,t) &\equiv \int D\eta\,\exp\left[-(1/4\kappa)\int_t^0 dt'[\dot\eta_a - v_a(\bar r+\eta,t')+v_a(\bar r,t')]^2\right]\\ &=\int D\eta\int Dp\,\exp\left[-\kappa\int_t^0 dt' p^2(t')\right]\exp\left[-i\int_t^0 dt' p_a[\dot\eta_a - v_a(\bar r+\eta,t')+v_a(\bar r,t')]\right]\ .\end{aligned} \tag{3.8}$$

The variable end point r' is introduced merely to allow a spatial derivative and we continue to define $\bar r(0)=0$ so that the boundary conditions on η become $\eta(0)=r'$ and $\eta(t)=r-\bar r(t)$. Integrate $p_a\dot\eta_a$ by parts and then Fourier-transform on the end point r via

$$\int d\eta(t)\exp\{iq[\bar r(t)+\eta(t)]\}\ ,$$

thereby obtaining

$\delta(p(t)-q)\exp[iq\bar{r}(t)]$.

We now introduce the linearization, i.e., expand $v(\bar{r}+\eta,t)$ to the first order in η. In this approximation the path integral over η is trivial and forces the semiclassical equation of motion (3.7b) on the $\vec{p}$ field:

$$G(r',0|q,t)\equiv e^{iq_a\bar{r}_a(t)}\int Dp\, e^{-\kappa\int_t^0 dt' p^2(t')} \times e^{i\vec{r}'\cdot\vec{p}(0)}\delta(\vec{q}-\vec{p}(t)) \times\prod_{t'}\delta(\dot{p}_a+\partial_a v_b(\bar{r}(t'))p_b) \ . \quad (3.9)$$

The path integral on p itself is now trivialized as the δ functions instruct one to initialize with $\vec{q}$ and integrate the equation of motion (3.7b) forward along the $\bar{r}(t)$ Lagrangian trajectory. This is accomplished by the formal but still useful expression

$$p_a(t')=M_{ab}(t',t)p_b(t) \equiv \mathcal{T}\{e^{-\int_t^{t'}dt'' m(t'')}\}_{ab}p_b(t) \ , \quad (3.10)$$

which involves a time-ordered product denoted by $\mathcal{T}$ (latest times on left) of the exponentiated strain matrix

$$m_{ab}\equiv\partial_a v_b(t)=\partial_a v_b(\bar{r}(t),t) \ .$$

The initial condition is $\vec{p}(t)=\vec{q}$. (Derivatives on $\vec{r}'$, which compute $\nabla\theta$, simply bring down factors of $\vec{p}(0)$ so in this section and in Sec. III which are devoted to the scalar PDF we set $r'=0$.) Collecting factors and suppressing the final-space time point,

$$G(q,t)=e^{i\vec{q}\cdot\vec{\bar{r}}(t)}e^{-(\kappa/2)\int_t^0 dt' p^2(t')} \equiv e^{i\vec{q}\cdot\vec{\bar{r}}(t)}e^{-(\kappa/2)\vec{q}\cdot\Sigma\cdot\vec{q}} \ , \quad (3.11)$$

where the second equality and the linearity of (3.10) suffice to define matrix Σ.

The behavior of the linearized G reduces essentially (to an extent we quantify below) to the study of $M_{ab}(0|t)$ computed along the Lagrangian trajectory. Provided the Lagrangian trajectory traverses many correlation volumes, $t/\tau\gg1$, as in the white velocity limit, M is the product of many uncorrelated and random matrices with unit determinant. The multiplicative ergodic theorem shows that an "averaged" Lyapunov exponent can be defined as

$$\bar{\gamma}_L=\lim_{t\to+\infty}\frac{1}{2t}\ln\{[\mathbf{M}(t|0)p(0)]^2/p^2(0)\} \ ,$$

where the limit exists for almost all directions of $p(0)$ [21]. We cannot take the infinite time limit, nor do we want to average at this stage since it will be precisely the fluctuations of the norm of $\mathbf{M}(0|t)$, $\|\mathbf{M}\|$, which are of interest. We therefore define a v-dependent Lyapunov exponent $\gamma_L(v)$ by

$$\|\mathbf{M}\|\sim e^{\gamma_L|t|} \ . \quad (3.12)$$

Its order of magnitude is $\sim\tau\|\partial v\|^2$ or $\sim D\xi^{-2}$ in the white-noise limit with D given by (3.4). Via (3.10), γ_L governs the growth of all wave vectors (forward in time from t to 0) along the Lagrangian trajectory except those initially perpendicular to the most expanding direction of $\mathbf{M}$. Exponent γ_L controls the divergence of classical trajectories with $\eta(0)$ fixed and $p(t<0)=q$ variable. The adjoint of $\mathbf{M}$ governs the separation of nearby Lagrangian trajectories as one goes from 0 to t, i.e., backward in time.

The linearization that leads to (3.11) is only valid for $t<t_*$ or $\eta<\xi$. (It is at this point where the single-scale assumption on v is essential.) Clearly, for short times and small κ, $\kappa q\cdot\Sigma\cdot q$ is $\ll1$ for $|q|\sim\xi^{-1}$ so $G(0,0|rt)$ is well localized near the Lagrangian trajectory. Thus we can estimate t_* by using (3.12) to reexpress Σ:

$$t_*\sim\tfrac{1}{2}\gamma_L^{-1}(v)\ln[\gamma_L(v)\xi^2/\kappa] \quad (3.13)$$

or, equivalently, $|G(q\sim\xi^{-1},t_*)|\sim\frac{1}{2}$. Replacing γ_L by $\bar{\gamma}_L$, (3.13) would yield the conventional estimate for the time a random strain field takes to stretch and fold a blob $\sim\xi$ down to a scale on which molecular mixing predominates. (The dependence of p^2 in (3.10) on $\vec{q}$ is shown below to be immaterial for the purposes of this section.)

The exponential growth in (3.12) greatly facilitates approximations, e.g., $r_*\sim\bar{r}(t_*)$, in (3.5), since the arbitrariness in the definition of t_* occurs inside a log, and r_* is only algebraically dependent on t_*, i.e., $\langle r_*^2\rangle\sim2Dt_*$. Of course, for $|t|>t_*$, our linear approximation absurdly overestimates the domain sampled by $G(0,0|r,t)$, making it grow exponentially out, whereas it should follow (3.6); once two points are separated by more than ξ, the distance between them grows only diffusively. This is not, however, a significant source of error in (3.5) since the integral terminates at t_* anyway, i.e., once $G(0,0|rt)$ is spread over $\Delta r>\xi$, the integral on r over $\vec{v}$ averages to zero.

To further validate the approximation that the distribution of θ is identical to that of $x(t_*)$, as follows from (3.5), we quantify the extent to which $|G(q,t)|^2$ (with $q^2=1$) is approximated by a step function $\Theta(t+t_*)$ and at the same time find the PDF of t_*. Let us study the moments

$$Q_n(T)\equiv\langle|G(q,t)|^{2n}\rangle|_{t=-T}=\langle e^{-2n\kappa\int_{-T}^0 dt\, p^2(t)}\rangle \ , \quad (3.14)$$

where $T>0$, $\vec{p}(t)$ is given by (3.10) with initial condition $\vec{p}(-T)=\vec{q}$, and $q^2=1$. Note that the absolute value in the definition of Q_n in (3.14) removes the $\bar{r}(t)$-dependent phase factor [see Eq. (3.11)], which upon averaging over the Lagrangian trajectories would have reduced $\langle G^n(q,t)\rangle$ to a Gaussian form even for short times $t<t_*$. In the white-noise limit $\tau\to0$, we assume that the strain matrix $\mathbf{m}(t)$ in (3.10) is uncorrelated with $\bar{r}(t)$, which remains fixed throughout, and replace the $\vec{v}(r,t)$ ensemble average by the Gaussian average over strain:

$$\langle\cdots\rangle=\mathcal{N}^{-1}\int D\mathbf{m}\,\delta(\mathrm{Tr}\mathbf{m})\exp\left[-(1/\sigma)\int dt\,[\mathrm{Tr}\mathbf{m}^+\mathbf{m}+\frac{1}{d+1}\mathrm{Tr}\mathbf{m}^2]\right]\cdots \ . \quad (3.15)$$

There is only one free parameter in (3.15) since we have assumed $\vec{v}$ is isotropic and homogeneous so that

$$\langle \partial_a v_b \partial_c v_d \rangle \sim \frac{\sigma}{2d}\frac{d+1}{d+2}[(d+1)\delta_{ac}\delta_{bd} - \delta_{ab}\delta_{cd} - \delta_{ad}\delta_{bc}] . \tag{3.16}$$

Rewrite (3.14) in discrete time with the insertion of a dummy path integral over $p^2(t)$:

$$Q_n = \mathcal{N}^{-1}\int D\mathbf{m}\,\delta(\mathrm{Tr}\mathbf{m})\exp\left[-\frac{\Delta}{\sigma}\sum_{j=0}^{N}[\mathrm{Tr}\mathbf{m}^+(j)\mathbf{m}(j) + \mathrm{Tr}\mathbf{m}^2]\right] \times \left\{\prod_{j=1}^{N}\int dp^2(j)\delta(p^2(j) - p^+(j-1)e^{\Delta m^+(j)}e^{\Delta m(j)}p(j-1))e^{-2n\kappa\Delta\sum_{j=0}^{N}p^2(j)}\right\} , \tag{3.17}$$

where $p(j) \equiv p(j\Delta - T)$, $p(N) = p(0)$, and the argument of the δ function enforces (3.7b). The integration over $\mathbf{m}$ performed in Appendix A leads to a much simpler path-integral expression,

$$Q_n = \mathcal{N}^{-1}\int Dx\, e^{-\frac{1}{2}\int_{-T}^{0}dt(\dot{x}-\gamma)^2} e^{-2n\kappa\int_{-T}^{0}dt\, e^{2x}} , \tag{3.18}$$

where we have defined $x(t) = \frac{1}{2}\ln p^2(t)$ and $\gamma = (d+6)/2$. [The time scale has been adjusted to eliminate the strain variance σ introduced in (3.15)]. Note that (3.18) substantiates several heuristic claims made above, namely, that the mixing time defined by $|G(q,t_*)|^2 \sim \frac{1}{2}$ can be estimated from $\mathbf{M}(0|t)$ and that the exceptional values of $\hat{q}$ for which p^2 does not grow according to (3.12) are immaterial.

By deriving Eq. (3.18), we have shown that $p^2(t)$ is governed by a log-normal ensemble with the secular growth rate $\partial_t \langle \ln|p| \rangle = \gamma$. This growth rate was previously identified with the average Lyapunov exponent as given by the multiplicative ergodic theorem for the product of random matrices. Note that $\gamma \sim d$ for large d, corresponding to the increase of the ratio of the secular growth rate to σ in (3.14). The evolution and statistics of $\vec{p}$ are the same as that for the "wave number" of the advected scalar structure discussed by Kraichnan [10] and the log-normal ensemble of Eq. (3.18) makes contact with his analysis.

The one-dimensional path integral in (3.18) is computed by observing that the term linear in $\dot{x}$ integrates to the boundary and the rest corresponds to the motion of a quantum particle in the potential e^{2x}. We have

$$Q_n(T) = e^{-(\gamma^2/2)T}\int dx\, e^{\gamma x}\mathcal{G}_n(x|T) , \tag{3.19}$$

where $\mathcal{G}_n(x|t)$ solves

$$[\partial_t - \tfrac{1}{2}\partial_x^2 - n\kappa e^{2x}]\mathcal{G}_n(x|t) = \delta(t)\delta(x) . \tag{3.20}$$

The RHS of (3.19) was normalized so that $Q_{n=0} = 1$. Equation (3.20) is solved in Appendix B by performing a Laplace transformation in t and noting that the substitution $z = e^x$ reduces the left-hand side (LHS) to the Bessel equation. The result for $T \gg 1$ is

$$Q_n(T) \approx \mathrm{const} \times T^{-3/2}e^{-(\gamma^2/2)}(2n\kappa)^{-\gamma/2}K_0(2n\kappa) , \tag{3.21}$$

which is valid for $T \gg \ln(n\kappa)^{-1}$ [the restriction being imposed by the asymptotic expansion in (B7)]. The rather minimal dependence of $\langle |G(q,-T)|^{2n} \rangle$ on n confirms the step-function character of $G(q,-T)$. The probability distribution of t_*, $\mathcal{P}(t_*)$, is then defined by

$$-\partial_T \langle |G(q,-T)|^2 \rangle = \int dt_* \delta(T - t_*)\mathcal{P}(t_*) = \mathcal{P}(T) , \tag{3.22}$$

where $\mathcal{P}$ is positive since $\langle |G|^2 \rangle$ is monotone decreasing and is properly normalized by virtue of $|G(q=0)|^2 = 1$. Thus, from Eq. (3.20) for $t_* \gg \langle t_* \rangle \sim \ln\kappa^{-1}$,

$$\mathcal{P}(t_*) \sim \frac{\gamma^2 e^{-(\gamma^2/2)t_*}}{t_*^{3/2}} + \cdots , \tag{3.23}$$

i.e., t_* is asymptotically exponentially distributed.

A few remarks concerning the physics of $\mathcal{P}(t_*)$ and the range of validity of (3.23) are in order. The calculation that culminated in Eq. (3.23) was a quantitative estimate of the probability of a configuration of a random velocity field leading to a large scalar fluctuation. These configurations have a Lagrangian trajectory with low strain. A crude estimate for the probability of $t_* = T$ can be obtained by requiring the strain at each point of the trajectory to be less than T^{-1}, which would guarantee that $p^2(t)$ remains of $O(1)$ and, hence, negligible dissipation. Assuming an $O(1)$ correlation time for $\mathbf{m}$ along the Lagrangian path then yields

$$(1/T)^T = \exp(-T\ln T)$$

as an estimate of the probability of such a configuration. This implies a $\mathcal{P}(t_*)$ decaying a little faster than exponential. This simple argument, however, underestimates the number of allowed configurations by suppressing the fluctuations of strain along the trajectory, which are properly accounted for in (3.17) and (3.18).

A minor caveat on (3.23) will be noted. No matter what happens with the strain, the lifetime of the fluid parcel cannot be extended beyond $\kappa^{-1} = \mathrm{Pe}$ since there is no way to eliminate the molecular diffusion. The error can be traced to the passage from (3.14) to (3.18) where for certain improbable trajectories we allowed

$$\int_{-T}^{0} dt \exp(2x) \sim O(1)$$

rather than $\geq O(T)$. Fortunately, this shortcoming in our derivation only matters for $\theta \sim \kappa^{-1}$ when $P(\theta)$ is already absurdly small.

The reader should now appreciate the warning given at the end of Sec. II regarding the turbulent diffusivity. Tails of the $P(\theta)$ arise only inasmuch as the mixing time t_* can be increased beyond its average value of order lnPe and up to Pe by controlling the strain. For large Re, if the various scales of velocity all fluctuate independently, they all have to be suppressed to achieve a lifetime $\gg 1$, which then occurs with vanishing probability. [Note that for a fully turbulent flow the mixing time based on cascade ideas is $O(1)$ rather than lnPe.] We will argue in the Conclusion that the eddy diffusivity fluctuates with the large-scale strain in the same way as the scalar lifetime, so that our approximation remains valid.

A final comment is due regarding our assumption that the velocity has negligible weight for $q \ll 1$. We have focused on the suppression of mixing to generate the tails and in Sec. IV will assume that the Lagrangian displacement is Gaussian for long times. One could also ask whether the probability of jetlike configurations of the velocity field is large enough to influence the tails. The answer is clearly no if the velocity is confined to a wave-number shell and remains so even if the wave number is thermal, which is an overestimate for real turbulence.

IV. SCALAR PDF

If one accepts the conclusion drawn from (3.21), namely, that $G(qt)$ behaves like $\Theta(t+t_*)$, then, via (3.1) and (3.5), the θ PDF is identical to that of $\bar{x}_*$. The latter is Gaussian and diffusive with D given by (3.4) provided the distances involved are $\gtrsim \xi$. Hence, knowing the distribution of t_* from (3.23), one readily derives

$$P(\theta) \sim \int_0^\infty dt_* \frac{e^{-\gamma^2(t_*/2)}}{t_*^{3/2}} e^{-\theta^2/4Dt_*} \sim \frac{1}{|\theta|} e^{-\gamma|\theta|/\sqrt{2D}} , \qquad (4.1)$$

valid for θ^2 larger than the variance

$$\langle \theta^2 \rangle \sim 2D \langle t_* \rangle \sim 2D \ln(\kappa^{-1}) .$$

We again see that the tails in $P(\theta)$ originate from the exponential probability of low strain trajectories leading to long lifetimes t_*.

It is very instructive to recompute $P(\theta)$ directly from the definition (3.1) via the characteristic function (2.5):

$$\hat{P}(\lambda) = \left\langle \exp\left[i\lambda \int_{-\infty}^0 dt \int dr\, v_x(x,t) G(0,0|rt) \right] \right\rangle , \qquad (4.2)$$

and not introduce t_* by hand. The exact expression (4.2) involves correlations between G's at different times, whereas (3.14) and its sequel did not. We will still neglect the correlations between the Lagrangian trajectory $\vec{r}(t)$ and the strain matrices $\mathbf{m}(t)$, which enter the linearized G, and v_x. This is most plausible for Gaussian white $\vec{v}$ and large dimensional space, but should be reasonable for any Gaussian $\vec{v}$ for $t_* \gg \tau$. With

$$\langle v_x(rt), v_x(r't') \rangle = \delta(t-t') D(r-r') ,$$

one has

$$\hat{P}(\lambda) = \left\langle \exp\left[-\lambda^2 \int_{-\infty}^0 dt \int dq\, D(q) |G(q,t)|^2 \right] \right\rangle = \left\langle \exp\left[-\lambda^2 \int_{-\infty}^0 dt \int dq\, D(q) e^{-2\kappa \int_t^0 dt' p^2(t'|t)} \right] \right\rangle , \qquad (4.3)$$

where we use $\vec{p}(t'|t)$ for the momentum in (3.10) to emphasize the boundary condition $\vec{p}(t|t)=\vec{q}$. For the velocity field (2.2), $D(q)$ is nonzero only for $q^2 \approx 1$ (in the scaled units) and $\int dq\, D(q) \sim \tau V^2$, i.e., eddy diffusivity. Equation (4.3) reduces to (4.1) provided $t_* = \int_{-\infty}^0 dt |G(q,t)|^2$ for $q^2 \approx 1$, which is, of course, consistent with thinking of $|G(q,t)|$ as the step function advocated earlier.

We now recompute the PDF. The idea is again to reduce it to a path integral on p^2 as in (3.17). Two technical difficulties are encountered, as follows.

(i) The $\int dt$ in (4.3) requires averaging $G(q,t)$ at different times which are not independent; the problem manifests itself in the appearance of the $p^2(t'|t)$ function with the $\vec{p}(t|t)=\vec{q}$ boundary conditions applied at different points with respect to the Lagrangian trajectory.

(ii) The $\int dt'$ integral appearing in the second exponential makes the path integral nonlocal in time, which would in general require the introduction of an additional field.

The issue of boundary conditions requires careful examination of the q dependence of $|G(q,t)|^2$. Let $\mathbf{Q}_{ab} \equiv q_a q_b$ so that

$$\frac{1}{2\kappa} \ln|G(q,t)|^2 \approx -\int_t^0 dt' \, \mathrm{Tr}[\mathbf{M}^+(t',t)\mathbf{M}(t',t)\mathbf{Q}] . \qquad (4.4)$$

Since

$$\mathbf{M}^+(t',t)\mathbf{M}(t',t) = R^+(t',t)\, \mathrm{diag}(t',t) R(t',t) ,$$

where the rotation matrices $R(t',t)$ for different t' are statistically independent if $\mathbf{m}$ is white and the largest eigenvalue of the diagonal matrix $\mathrm{diag}(t',t)$ is $e^{\gamma|t-t'|}$, the integral on t' then contains many terms of comparable magnitude but involving uncorrelated $R(t',t)$ matrices. Thus we expect the RHS to be independent of the direction of the $\vec{q}$ vector [22], i.e., independent of $\mathbf{Q}$. Also, since for most velocity configurations the integrand grows exponentially with t', we expect the RHS to be dominated by the upper limit of integration. The latter suggests a "local" approximation for the dissipation integral in (4.3) where it is estimated from the value of the integrand $p^2(t'|t)$ at the upper limit $t'=0$. The validity of such an approximation is quantified in the course of computing $\langle |G|^n \rangle$ in Appendix B.

We are thus led to the approximate expression

$$\ln|G(q,t)|^2 \approx -2\kappa p^2(0|t) \approx -2\kappa \, \mathrm{Tr}\mathbf{M}^+(0,t)\mathbf{M}(0,t) . \qquad (4.5)$$

Denoting $p^2(t) \equiv p^2(0|t)$, we rewrite (4.3) as

$$\hat{P}(\lambda) = \langle e^{-\lambda^2 D \int_{-\infty}^0 dt\, e^{-2\kappa p^2(t)}} \rangle . \qquad (4.6)$$

Using (4.5) for $p^2(t)$, we repeat the derivation in Appendix A to arrive at the "Abelian" path integral [in units such that $D=\frac{1}{2}$ and normalized to $\hat{P}(0)=1$ as in (3.19) and (3.20)]

$$\hat{P}(\lambda)=\int Dx\, e^{-\frac{1}{2}\int_{-\infty}^{0}dt(\dot{x}-\gamma)^2}e^{-(\lambda^2/2)\int_{-\infty}^{0}dt\, e^{-2\kappa e^{2x}}}$$
$$=\lim_{T\to\infty} e^{-\gamma^2 T/2}\int_{-\infty}^{\infty}dx\, e^{\gamma x}\mathcal{g}(x,T)\ , \qquad (4.7)$$

where $\mathcal{g}(x,t)$ solves

$$\left[\partial_t-\tfrac{1}{2}\partial_x^2+\frac{\lambda^2}{2}V(x)\right]\mathcal{g}(x,t)=\delta(t)\delta(x)\ , \qquad (4.8)$$

with $V(x)=e^{-2\kappa e^{2x}}$. The Green's function is solved for in Appendix C under a further (and mild) approximation that $\exp[-2\kappa\exp(2x)]$ can be replaced by a step function in x at $x_*\equiv\frac{1}{2}\ln\kappa^{-1}$, yielding

$$\hat{P}(\lambda)=\frac{2\gamma e^{(\gamma-\sqrt{\gamma^2+\lambda^2})x_*}}{\gamma+\sqrt{\gamma^2+\lambda^2}}+O(T^{-3/2}e^{-(\gamma^2/2)T}) \qquad (4.9)$$

in the large-T limit. (As discussed earlier, this expression, however, should not be extended beyond $T=\kappa^{-1}$.)

We observe that variance of the PDF $\langle\theta^2\rangle$,

$$\langle\theta^2\rangle=\langle\partial_\lambda^2 Z\rangle|_{\lambda=0}\sim\gamma^{-1}x_*\ ,$$

which is $O(\ln\kappa^{-1})$. This agrees with the naive "mean-field" estimate which followed (4.1). On the other hand, $\hat{P}(\lambda)$ has a strip of analyticity in the complex λ plane of width γ which implies exponential tails for its Fourier transform, the scalar PDF, $P(\theta)\sim e^{-\gamma|\theta|}$. This suggests a simple *ad hoc* crossover formula matching the two limits of the PDF:

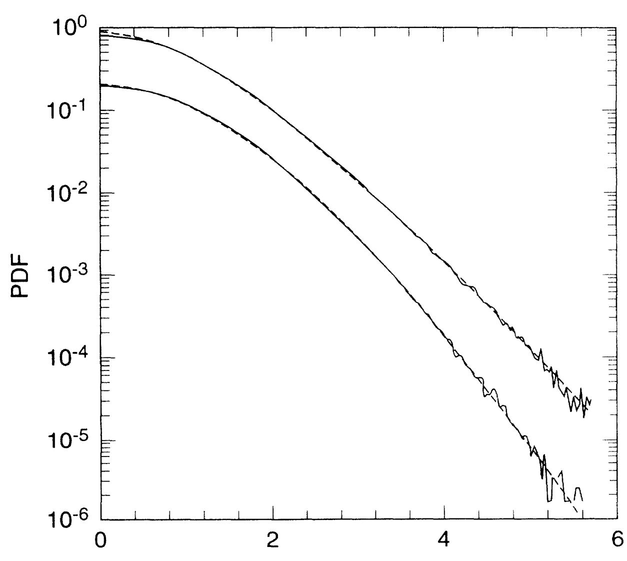

FIG. 1. The scalar PDF in three dimensions computed from (4.3) using the correct time-integrated dissipation (lower curve) versus an approximation using the local dissipation (4.5) as explained in the text. The dashed curves are fits to (4.10), the data sets are offset for clarity, the variance is scaled to unity, and $\kappa=0.01$ through all values ≤ 0.1 gives identical PDF's.

$$P(\theta)\sim e^{-\gamma\theta^2/(\ln\kappa^{-1}+|\theta|)}\ . \qquad (4.10)$$

In principle, of course, $P(\theta)$ is determined directly by the Fourier transform of (4.9) from which one can easily establish the asymptotic result $P(\theta)\sim|\theta|^{-1/2}e^{-\gamma|\theta|}$ [cf. (4.1)].

The more significant approximations employed in this section after the point where G was linearized can easily be checked numerically. The "correct" PDF can be sampled by first evaluating (4.4) (with $\mathbf{Q}=1$) for one realization of the Gaussian white $\mathbf{m}$ ensemble (3.15). Following (4.2), we sample θ by computing $\int_{-\infty}^{0}dt\,\omega(t)G$, where $\omega(t)$ is an independent Gaussian white variable. The first approximation is then just to define a t_* where G first hits 0.5 and equate θ to a Gaussian with variance t_*. The result is indistinguishable from the "correct" calculation. The second approximation defines the t_* using the "local" G in (4.5). Figure 1 shows that both distributions are well fit by (4.10). All dependence on Pe for values $\gtrsim 10$ occurs through the variance.

V. SCALAR GRADIENT PDF

We now investigate the asymptotic behavior of the PDF of the scalar gradient defined by (2.4b). The corresponding generating function is

$$\hat{P}(\vec{\lambda})=\langle e^{i\lambda_a\partial_a\theta(0,0)}\rangle\ . \qquad (5.1)$$

The equation for the gradient of the scalar is obtained simply by differentiating (2.3),

$$[\partial_t+v_b\partial_b-\kappa\partial_b^2]\partial_a\theta+\partial_a v_b\partial_b\theta=\partial_a v_x\ . \qquad (5.2)$$

The essential difference here is the appearance of the straining term (the second one on the LHS) which describes amplification of the gradient by the spatially nonuniform flow field. Note that the small-scale cutoff for the scalar field is at $\xi\mathrm{Pe}^{-1/2}$—the length scale for which the advection and diffusion terms of (5.2) balance. Hence, expect $\langle(\partial\theta)^2\rangle\sim g^2\mathrm{Pe}$.

The solution of Eq. (5.2) can be written as

$$\partial_a\theta(0,0)=\int_{-\infty}^{0}dt\int dr\,\mathbf{G}_{ab}(0,0|r,t)\partial_b v_x(r,t)\ , \qquad (5.3)$$

with the matrix Green's function $\mathbf{G}_{ab}$ for the gradient defined by the path integral

$$\mathbf{G}_{ab}(0,0|r,t)=\int_{\substack{r(t)=r\\ r(0)=0}}\mathrm{D}r\, M_{ab}(0|r,t)e^{-S(r,t)/2\kappa}\ , \qquad (5.4)$$

with the same action $S(r,t)$ as in (3.2) and the strain history matrix $\mathbf{M}$ defined for the $r(t)$ trajectory by (3.10). While the gradient Green's function involves familiar objects, the approximations required to reduce it to a tractable linearized form are far more serious than for the scalar. We present two approximations making plain their deficiencies and then display their consequences numerically.

Both approximations begin with the observation that since for $|t|<t_*$ the paths contributing to the integral in (5.4) are localized close to the Lagrangian trajectory by the exponential of the action and since the $M_{ab}(0,0|r,t)$

varies with r only on the scale $\sim\xi$, one can evaluate the latter on the Lagrangian trajectory. This leads to

$$\mathbf{G}_{ab}(0,0|r,t)\approx M_{ab}(0|t)G(0,0|r,t) .$$

The external integral on r in (5.3) is then evaluated by linearizing $G(0,0|r,t)$ as in (3.8) and (3.11) and assuming that the spatial dependence of v_x cuts off the integral at $|r-\bar{r}(t)|\sim\xi$. As before [see Eq. (4.5)], the Fourier-transformed Green's function $G(q,t)$ with $|q|\sim\xi^{-1}$ appears and is approximated by

$$G(q,t)\approx \exp[iq\bar{r}(t)]G_0(t)$$

with

$$G_0(t)\equiv \exp\left[-\kappa\int_t^0 dt'\,\mathrm{Tr}\mathbf{M}^+(t'|t)\mathbf{M}(t'|t)\right] . \quad (5.5)$$

We arrive at the approximate semiclassical expression

$$\partial_a\theta=\int_{-\infty}^0 dt\, M_{ab}(0|t)\partial_b v_x(\bar{r}(t),t)G_0(t) . \quad (5.6)$$

Now, to generate the *first* approximation, we note that

$$\partial_t M_{ax}(0|t)=M_{ab}\partial_b v_x(\bar{r}(t),t)$$

so that integrating the RHS of (5.6) by parts yields

$$\partial_a\theta=\delta_{ax}-\int_{-\infty}^0 dt\, M_{ax}(0|t)\partial_t G_0(t) . \quad (5.7)$$

Note that $\partial_a\theta-\delta_{ax}$ is nothing but the gradient of the total unshifted temperature, i.e., $\partial_a T$. Our extensive approximations have preserved the mean value of the gradient, as follows from the fact that in the white-noise limit, $\langle M_{ax}(0|t)\rangle=\delta_{ax}$, so that the average of $\partial_a T$ is $-\delta_{ax}$. Thus, Eq. (5.7) knows about the large-scale boundary conditions and can be expected to capture correctly the skewness of the gradient PDF. Finally, note that (5.7) is very analogous to the form the scalar assumed when expressed in terms of t_*. To the extent that $G_0(t)$ behaves like a step function, its derivative is a δ function at t_* [cf. (3.21)].

Analytic work with (5.7) would be quite arduous, as the simple approximation which follows demonstrates, and we content ourselves with a numerical computation of the gradient PDF based on (5.7). We sample $M_{ab}(t'|t)$ by exponentiating a string of $\partial_a v_b$ matrices drawn from a Gaussian ensemble defined by (3.15) and (3.16). The time slice is made small enough so as to be in the white limit and verify $\langle M_{aa}\rangle=1$. The result is shown in Fig. 2(a) for $\kappa=10^{-4}$ for $d=3$: Note a conspicuous cusp in the center and a crossover to exponential tails beyond the variance of the PDF. For $d=2$, the tails are slightly more stretched, but the center cusp is the same. The Figure is virtually indistinguishable if one replaces $\partial_t G_0$ by $\delta(t-t_*)$, where t_* is determined by when

$$\kappa\int_t^0 dt'\,\mathrm{Tr}\mathbf{M}^+(t'|t)\mathbf{M}(t'|t)$$

first reaches ~ 1. Replacing $2\ln G_0$ by the end-point value of the integrand $\kappa\,\mathrm{Tr}\mathbf{M}^+(0|t)\mathbf{M}(0|t)$ as we have done in computing the scalar PDF significantly narrows the wings of the gradient PDF but leaves them asymptotically exponential and the center cusped. The PDF in this "local" approximation for dissipation is compared with that based directly on (5.7) in Fig. 2(a). The PDF is noticeably skewed for $\kappa=0.01$ [see Fig. 2(b)] and the normalized skewness appears to scale as $\mathrm{Pe}^{-0.3\pm0.1}$ in both two and three spacial dimensions. Note that while $\langle\partial_x\theta\rangle=0$, the peak of $P(\partial_x\theta)$ moves with increasing Pe

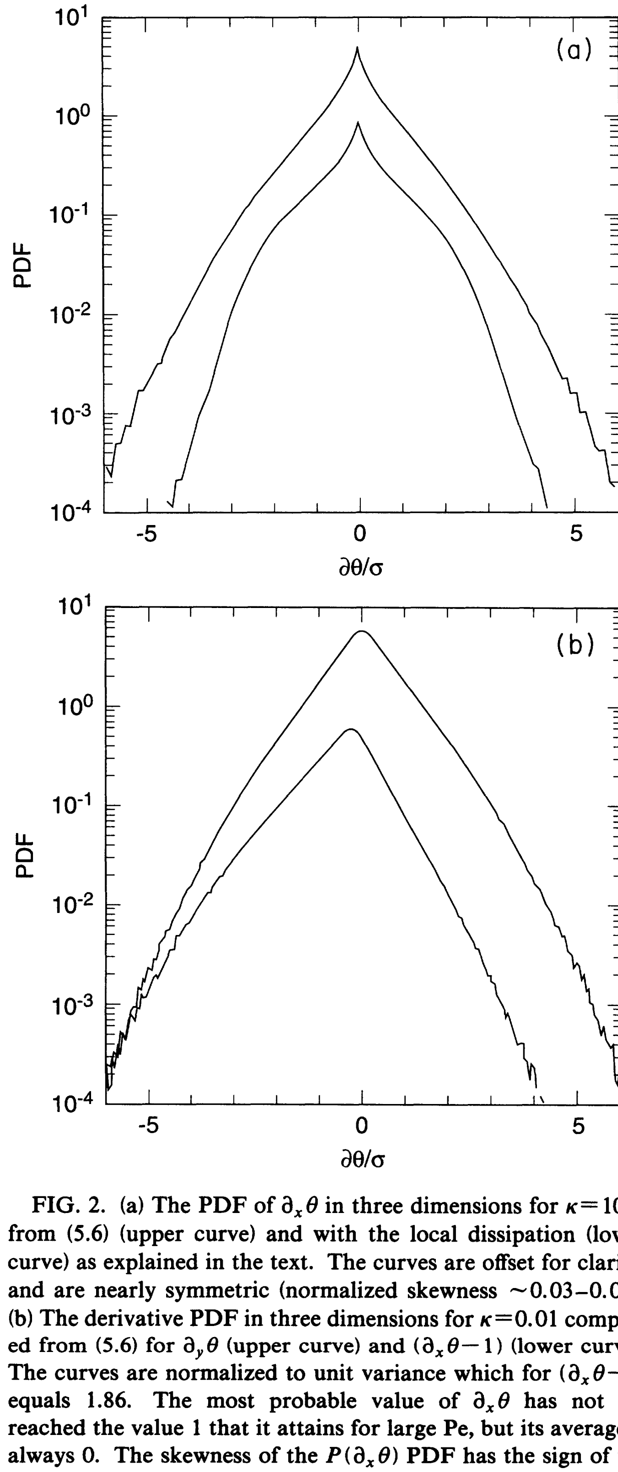

FIG. 2. (a) The PDF of $\partial_x\theta$ in three dimensions for $\kappa=10^{-4}$ from (5.6) (upper curve) and with the local dissipation (lower curve) as explained in the text. The curves are offset for clarity, and are nearly symmetric (normalized skewness $\sim$0.03–0.06). (b) The derivative PDF in three dimensions for $\kappa=0.01$ computed from (5.6) for $\partial_y\theta$ (upper curve) and $(\partial_x\theta-1)$ (lower curve). The curves are normalized to unit variance which for $(\partial_x\theta-1)$ equals 1.86. The most probable value of $\partial_x\theta$ has not yet reached the value 1 that it attains for large Pe, but its average is always 0. The skewness of the $P(\partial_x\theta)$ PDF has the sign of the large-scale gradient. The upper PDF was prepared from a histogram for $|\partial_y\theta|$ and then reflected about zero since the off-diagonal elements of $\mathbf{M}(0|t)$ are symmetric.

towards $\partial_x \theta = 1$, which corresponds to $\partial_x T = 0$ and hence to the preponderance of the fully mixed regions [20]—the gradient expulsion effect.

It is useful to compare the above direct numerical evaluation of the gradient PDF based on (5.7) with a simple mean-field-type approximation for the same equation. The latter approximation corresponds to replacing $\partial_t G_0(t)$ on the RHS of (5.7) by $\delta(t - t_*)$ with t_* *fixed* at its average value $\sim \ln\text{Pe}$ [see (3.13)]. Within this approximation $\partial_a T \approx -M_{ax}(0|t_*)$ and its statistics can be obtained by studying the PDF of vector $p_a(t) \equiv M_{ax}(t|0)$, since the statistics of $M_{ab}(t'|t)$ depends on $t'-t$ only. For Gaussian white strain, $\mathbf{m}(t)$, distributed according to (3.15) and (3.16), the PDF of $\vec{p}$, $\Omega(\vec{p},t)$, is governed by

$$\partial_t \Omega(\vec{p},t) = (d+1)\frac{\partial^2}{\partial p^2}[p^2 \Omega(\vec{p},t)] - 2\frac{\partial^2}{\partial p_a \partial p_b}[p_a p_b \Omega(\vec{p},t)] , \tag{5.8}$$

which is obtained from a similar equation for the generating function derived by computing $\partial_t \langle \exp[i\vec{\zeta}\cdot\vec{p}(t)] \rangle$ using the "equation of motion" $\partial_t p_a = m_{ab} p_b$ and the white-noise correlator for $\mathbf{m}$ (3.16) which brings down from the exponent another factor of $\partial_t \vec{p}\cdot\vec{\zeta}$. Equation (5.8) with the initial condition $\Omega(\vec{p},0) = \delta(\vec{p} - \hat{x})$ can be readily solved. For $d=2$ the result is conveniently expressed in polar coordinates:

$$\Omega(r,\phi,t_*) = \frac{1}{\sqrt{\pi t_*}\, r} \sum_m e^{im\phi} e^{-(3m^2+1)t_*} e^{-(\ln^2 r)/4t_*} , \tag{5.9}$$

where $r \equiv |\vec{p}|$ and $\phi \equiv \tan^{-1}(p_y/p_x)$. This of course yields a log-normal distribution for the magnitude of $\vec{p}$: $\int d\phi |\vec{p}| \Omega(|\vec{p}|,\phi,t)$. However, the anomalously long tails of the gradient PDF predicted by this argument are not to be believed because the mean-field approximation underestimates the effect of diffusion on large gradients which was properly included in (5.7). The approximation is expected to be more reliable for small gradients, i.e., the center of the PDF. Therefore, we compute the curvature at the center of

$$P(p_y) = \int d\phi \int dr\, r\Omega(r,\phi,t_*)\delta(r\sin\phi - p_y)\delta(r\cos\phi) .$$

We find that as $p_y \to 0$,

$$\partial^2 \ln P(p_y) \to e^{4t_*} \sim \text{Pe}^{1/2}$$

to the leading order in Pe. The scaling with Pe in this expression is obtained by comparing it to $\langle p^2 \rangle$ which is equal to e^{8t_*} as computed from (5.9) but is also known to be $\sim$Pe, which effectively fixes the mean-field cutoff t_* in terms of Pe. As a result, the curvature at the tip of $\ln P(\partial_y \theta)$ as in Figs. 2(a) and 2(b) is a factor of $\text{Pe}^{3/2}$ greater than that for a Gaussian PDF with the same variance. This at least qualitatively explains the cuspy appearance of the gradient PDF function at large Pe.

The mean-field theory (MFT) for the gradient PDF also yields an estimate for the gradient skewness. Integrating (5.8) over $\vec{p}$ with a $p^2 p_x$ weight factor results in an equation for the third moment of Ω at time t:

$$\partial_t \ln\langle p^2 p_x \rangle = 2(d-1)(d+4) .$$

Hence,

$$\langle p_x^3(t_*) \rangle \sim \exp[2(d-1)(d+4)t_*] ,$$

which should be compared to the variance

$$\langle p^2 \rangle \sim \exp[(2d^2+2d-4)t_*] \sim \text{Pe} ,$$

computed by similar means. Thus the normalized derivative skewness $S \sim \text{Pe}^{-\zeta}$ with exponent

$$\zeta = (d^2 - 3d + 2)/(2d^2 + 2d - 4) .$$

For $d=2$, we have $\zeta=0$, while for $d=3$, $\zeta=0.1$. In both cases the exponent is smaller than the 0.3 ± 0.1 value found numerically for (5.7), indicating that the MFT is overestimating the skewness. In the $d\to\infty$ limit where naively one may expect the MFT to work best, it predicts $\zeta \to \frac{1}{2}$, which, however, is difficult to check numerically.

Our second scheme for reducing (5.3) attempts to retain the proper dissipative cutoff for large gradients but is more cavalier regarding the correlations between the source v_x and the strain so that it loses the anisotropic aspects of the gradient fluctuations and, consequently, the skewness. Here we compute $\hat{P}(\vec{\lambda})$ directly from (5.3) by performing a Gaussian average over v_x and use isotropy to arrive at the expression depending on λ^2 only:

$$\hat{P}(\vec{\lambda}) \simeq \left\langle \exp\left[-\lambda^2 \int_{-\infty}^{0} dt\, \text{Tr}\mathbf{M}^+(0|t)\mathbf{M}(0|t) \exp\left[-2\kappa \int_t^0 dt'\, \text{Tr}\mathbf{M}^+(t'|t)\mathbf{M}(t'|t) \right] \right] \right\rangle \tag{5.10}$$

(with suitably scaled λ). We, again, for the sake of simplicity, resort to a local approximation for the dissipation and repeating Eqs. (4.6) and (4.7) arrive at

$$\hat{P}(\vec{\lambda},T) = \int Dx\, e^{-\frac{1}{2}\int_T^0 dt(\dot{x}-\gamma)^2} e^{-(\lambda^2/2)\int_T^0 dt\, V(x)} = e^{-(\gamma^2/2)T} \int dx\, e^{\gamma x} \tilde{\mathcal{G}}(x,T) , \tag{5.11}$$

with the Green's function $\tilde{\mathcal{G}}(x,T)$ solving

$$\left[\partial_t - \tfrac{1}{2}\partial_x^2 + \frac{\lambda^2}{2} V(x) \right] \tilde{\mathcal{G}}(x,t) = \delta(t)\delta(x) , \tag{5.12}$$

with the effective potential

$$V(x) \equiv e^{2x} e^{-\kappa e^{2x}} \approx e^{2x} \Theta(x_* - x) , \tag{5.13}$$

where as before we will approximate the double exponential by the $x_* \approx \frac{1}{2} \ln \kappa^{-1}$ cutoff.

We "solved" for $\hat{P}(\vec{\lambda})$ in Appendix D by reducing it to a blitz of Bessel functions. One again finds an analyticity strip in λ and thus exponential tails. To actually display the PDF described in (5.11), it is the easiest, again, to make up a process whose characteristic function is (5.11) and sample it numerically. Thus we construct a free particle $x(t)$ and then sample

$$\int_T^0 dt \, V^{1/2}[x(t)] \omega(t) ,$$

where $\omega(t)$ is Gaussian and white. The histogram is shown in Fig. 3 for the two limits: $\gamma T \ll x_*$ and $\gamma T \gg x_*$, with $\gamma T \gg T^{1/2}$ in both cases. When the cutoff is supplied by the diffusivity, the distribution is nicely exponential, while in the opposite limit where one takes $\kappa \to 0$ with T fixed, the output is consistent with lognormality. The latter is not surprising since except for the time integral on $V(x)$, (5.11) defines a log-normal distribution (see also Appendix B).

A significant conclusion which obtains in spite of our approximations is that lognormality disappears in a steady state under dissipation. This is certainly the case in the "toy model" represented by (5.11) where the crossover from lognormal to exponential tails occurs as x_* becomes smaller than γT. The physics is, of course, that the dissipation acts first on the largest values of the gradient, so that one is never looking at an unconstrained product. We also insist on continuous injection or forcing, which is essential for maintaining the steady state.

There are many deficiencies in our modeling of dissipation that are much more apparent for the derivative than for the scalar. Retaining the buildup in dissipation over time is necessary, as we showed with our first approximation. Also important was the correlation between the source and the strain which was at the origin of the derivative skewness. A more complete treatment of the problem should also include the correlation of the strain and velocity along the Lagrangian trajectory. Specifically, for a static velocity field, the Lagrangian derivative of $v_a p_a$ is zero, so that only the components of $\vec{p}$, and hence components of the scalar gradient, *normal* to the Lagrangian trajectory can grow. This leads to the streaky patterns of the scalar and the alignment of the gradient perpendicular to the streamlines, as observed in the experiments.

Equations very similar to (5.2) have been analyzed by Kraichnan [10] in the context we are considering, although different compromises were made in their solution. He retained the time history in the dissipation but was more cavalier with the forcing. On the other hand, the analysis of Ott and Antonsen [13] concentrated on the spatial distribution of the gradient in the $\kappa=0$ limit and for the $\kappa \neq 0$ case did not address the fluctuations of dissipation. Majda [14] has found steady-state non-Gaussian statistics for the scalar in the presence of random shear (by a path-integral technique). Such a flow, unlike turbulent flows, has zero Lyapunov exponent.

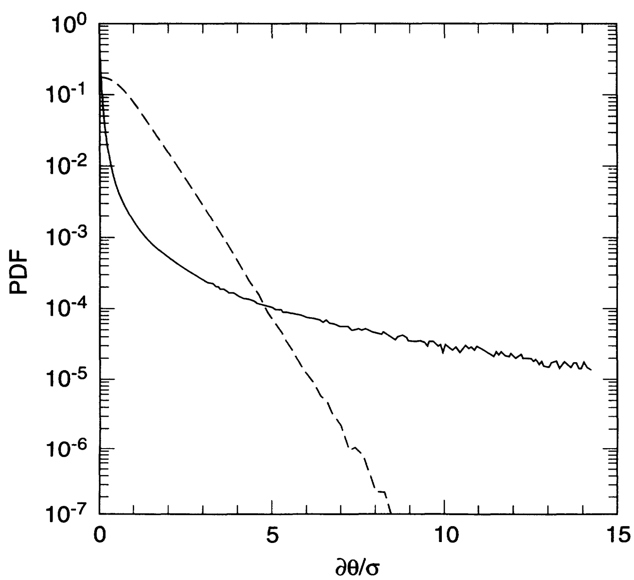

FIG. 3. The derivative PDF from (5.10) in the $\kappa=0$, finite-T limit (solid curve) and $\kappa > 0$, infinite-T limit (dashed curve).

VI. CONCLUSION

Tails in the distribution of a scalar advected by random flow arise very generally due to fluctuations in the *strain-enhanced mixing* which imparts an exponentially distributed lifetime to clumps of scalar drawn from distant values of the mean gradient. The Lagrangian displacement itself is a simple random walk as obtains for scales larger than ξ. Jetlike events in which the velocity is directed along the axis of a radius-ξ cylinder for a distance much greater than $\sqrt{\kappa t}$ have negligible probability (i.e., are dominated by the random walk), even if the velocity has an equipartition spectrum for long wavelengths which is an overestimate for turbulence. This mechanism is different from the one occurring in a discrete transport model [15,16,23] where instantaneous interchange of fluid parcels is allowed and tails in the scalar represent the Poisson distribution of interchanges within a dissipation time which is essentially fixed.

In our analysis of the scalar PDF several controlled and ultimately minor approximations were made in employing the dissipative cutoff. Several analytic variants, e.g., (4.5), and direct simulation (Fig. 1) all showed that instantaneously erasing the fluctuation of the scalar when the local gradient exceeded $\mathrm{Pe}^{1/2}$ was adequate. The white-noise approximation was unessential both because Lagrangian quantities would vary even if the Eulerian ones are frozen, and far enough in the tail, t_* is much greater than the Lagrangian correlation time, which is the real requirement. Our neglect of the correlation between the Lagrangian trajectory $\vec{r}(t)$ and the strain along it is more plausible in high spatial dimension, and the large-d expansion could in principle improve the rigor of the calculation. Clearly, the frozen $d=2$ velocity field is exceptional because of the lack of ergodicity of Lagrangian motion.

One of the key elements of our analysis has been the semiclassical approximation for the Green's function followed by the linearization about the Lagrangian trajectory. This is reasonable for a single-scale random flow with $\mathrm{Pe} \gg 1$, but would be more difficult to justify the $\mathrm{Re} \gg 1$ turbulent flow with its multiscale velocity field and effective $\mathrm{Pe} \sim 1$ because of eddy diffusivity. In the latter case the crucial question is whether controlling the large-scale strain will control the mixing time of the $\sim \xi$ blob of scalar. Such a requirement—or assertion—is at variance with simple notions that postulate a homogeneous, nonfluctuating contribution to the eddy diffusivity from each decade of velocity scales irrespective of how they are being driven. We prefer to think that everything is contingent on the largest scales of motion. At the present time, the most compelling arguments for our point of view are the laboratory experiments [1–6].

The gradient PDF is complementary to the scalar one in that it samples the small scales rather than $\sim \xi$. The velocity spectrum and Prandtl number certainly do matter for the gradient, and our calculation is strictly limited to the Batchelor regime. The gradient PDF depends in an essential way on the steady-state balance between stretching and dissipation. Although $\mathbf{M}(0|t)$ is lognormally distributed for fixed t, the dissipation depends on $\mathbf{M}$ having a larger effect for larger values of $\mathbf{M}$ and eventually resulting in a merely exponential tail for the gradient PDF. The disappearance of lognormality in the steady state is also exemplified by (5.11), which in spite of its defects as a model of (5.1) clearly would be lognormal for T finite and $\kappa=0$ but is exponential in the physical limit of infinite T, $\kappa>0$. On the other hand, the exponential nature of the tail can be understood intuitively by assuming that the large gradients are a consequence of large jumps of the scalar field occurring over a *fixed* dissipation scale. Because of the exponential tail of the scalar PDF, we expect to have an exponential tail in the probability of large jumps and, hence, large gradients.

Another extension of the conventional log-normal wisdom was required to understand the cuspy structure of the center of the gradient PDF. The appearance of the cusp in the large-Pe limit can be at least qualitatively explained by the mean-field calculation of the PDF of the gradient *vector* which generalizes the usual log-normal distribution for the *magnitude* of the gradient.

A steady forcing provided by the imposition of a mean gradient is essential for clean conclusions. If the scalar were injected periodically, then for appropriate time scales there would be a window of lognormality for times early enough that the dissipation is not yet felt. A constant imposed gradient also generates the skewness which would be zero with isotropic initial data. In fact, the anisotropy of the small scales is described rather naturally by the Lagrangian formalism. For example, consider the correlation of the scalar gradient and the strain, $Y \equiv \langle \partial_a \theta \partial_b \theta \partial_a v_b \rangle$; the only contribution to Y comes from the latest τ segment of the Lagrangian trajectory in (5.3) and (5.4), so that in the white-noise limit

$$Y \sim \tau \langle (\partial v)^2 \rangle \langle (\partial \theta)^2 \rangle \sim D \xi^{-2} g^2 \mathrm{Pe} \, .$$

By a mild extension of our arguments in the Batchelor regime (still neglecting the correlation between velocity and strain), it is straightforward to display the distribution for the entire θ field. Specifically, for the generating functional $\hat{P}\{\lambda\}$,

$$\begin{aligned}\hat{P}\{\lambda\} &= \left\langle \exp\left[-i \int_{-\infty}^{0} dt \int \int dr' dr \, \lambda(r') G(r',0|rt) v_x(rt) \right] \right\rangle \\ &= \left\langle \exp\left[-D \int_{-\infty}^{0} dt \, G_0(t) \int dr_1 \int dr_2 \lambda(r_1) \lambda(r_2) \exp\{ -[r_{12} \mathbf{M}(0|t) \mathbf{M}^{+}(0|t) r_{12}]^{1/2} / \xi \} \right] \right\rangle . \end{aligned} \tag{6.1}$$

The second line follows for white noise v as in (4.3) or (5.10) whose spacial correlations are exponential (2.2). The final points $r_{1,2}$ which label λ are related via their respective Lagrangian trajectories to their locations at earlier times. As already remarked, the matrix $\mathbf{M}(0|t)$ which governs the growth of $\vec{p}$ forward in time governs the divergence of Lagrangian trajectories backwards in time, which explains its appearance in the exponential of (6.1). For $|r_{1,2}|$ larger than a dissipation length, the time integral is cut off by the decorrelation between the preimages of $r_{1,2}$ rather than by the diffusion.

A simple expression follows if we work in the Abelian limit as in (4.5) and (4.7):

$$\hat{P}\{\lambda\} = \int Dx \exp\left[-\tfrac{1}{2} \int_{-\infty}^{0} dt \, (\dot{x} - \gamma)^2 \right] \exp\left[-\int_{-\infty}^{0} dt \int \int dr_1 dr_2 \lambda(r_1) \lambda(r_2) e^{-|r_{12}| e^{x} - 2\kappa e^{2x}} \right] ; \tag{6.2}$$

with suitable choices of $\lambda(r)$ one can recover either (4.7) or (5.10). The correlation function $\langle \theta(r_1) \theta(r_2) \rangle$ can be correctly evaluated in the mean-field limit by replacing the time integral by $\gamma^{-1} \ln |r_{12}|^{-1}$ to obtain

$$\langle \theta(r_1) \theta(r_2) \rangle \sim -\ln |r_{12}|$$

or

$$\langle [\theta(r_1) - \theta(r_2)]^2 \rangle \sim \ln(r_{12}^2 / \kappa)$$

in agreement with Batchelor's result. Of course, (6.2) contains much more information and is the most succinct statement of solvability for the problem of advection by a single-scale velocity field.

An alternative approach to the statistics of the $\theta(\vec{r})$

field in the case of velocity field which is white in time is provided by the Hopf equations [24] for the multipoint correlation functions. These are obtained from the conditions for the statistically steady state:

$$\partial_t \langle T(r_1,t)T(r_2,t)\cdots T(r_N,t)\rangle = -\sum_{j=1}^{N} \langle [\vec{v}(r_j,t)\cdot\vec{\partial}_j - \kappa\partial_j^2] \times T(r_1,t)T(r_2,t)\cdots T(r_N,t)\rangle = 0 \ . \quad (6.3)$$

Since in the white-noise limit, $v(r,t)$ correlates only with the change in $T(r',t)$ in the latest τ segment, one arrives at a closed set of equations for equal-time correlators:

$$\sum_{i,j}^{N} [C_{ab}(r_i-r_j)\partial_i^a\partial_j^b + \delta_{ij}\kappa\partial_j^2]\langle T(r_1)\cdots T(r_N)\rangle = 0 \ , \quad (6.4)$$

where

$$C_{ab}(r) \equiv \int dt \langle v_a(r,t)v_b(0,0)\rangle \ .$$

Substituting $T(r)=\theta(r)+\vec{g}\cdot\vec{r}$ and using translational invariance of θ correlators leads to

$$\sum_{i\neq j}^{N} [D_{ab}(r_i-r_j)+\kappa\delta_{ab}]\partial_i^a\partial_j^b\langle \theta(r_1)\cdots\theta(r_N)\rangle = \sum_{i\neq j}^{N} g_a g_b C_{ab}(r_i-r_j)\langle\theta\cdots\rangle_{ij}^{N-2} + \sum_{i\neq j}^{N} g_a D_{ab}(r_i-r_j)\partial_j^b\langle\theta\cdots\rangle_i^{N-1} \ , \quad (6.5)$$

where we have defined $D_{ab}(r)\equiv C_{ab}(0)-C_{ab}(r)$ and used the notation $\langle\theta\cdots\rangle_i^{N-1}$ to denote the $N-1$st-order correlator at points r_j, with $j=1,\ldots,i-1,i+1,\ldots,N$. We observe that the left-hand side is related to the Richardson diffusion operator [24,25], while the RHS is the source term driven by the large-scale gradient.

The above equations are convenient for studying the low-order correlators and are valid for velocity fields with arbitrary spatial correlations (as long as the velocity field remains Gaussian and white). For example, for the two-point function, one readily recovers Batchelor's result [8] for the single-scale flow and the Corrsin-Obukhov [24] power-law behavior in the case of velocity field with algebraic decay of spatial correlations. [Curiously, the existence of scaling solutions of (6.5) is not accompanied by conformal invariance [26] properties even in $d=2$.] On the other hand, the use of (6.5) in the study of the PDF asymptotics is not immediately evident; by contrast, the Lagrangian path-integral formulation is more intuitively transparent.

Finally, it is readily apparent why multiscale advection is more complex than the single-scale Batchelor case: linearization of the velocity is no longer valid out to distances of the order of the velocity correlation length. We expect the Lagrangian Green's function to remain a useful construct, as already noted by Kraichnan [25]. Our contribution has been to think of it as a random quantity and evaluate it by path-integral methods.

ACKNOWLEDGMENTS

It is a pleasure to acknowledge stimulating interactions with M. Holzer, R. Kraichnan, and A. Pumir. E.D.S. was supported by the Air Force Office of Scientific Research under Grant No. 90-0090 and by NSF Grant No. DMR 9012974. This project was begun while E.D.S. was a visitor at the Rockefeller University and the Courant Institute, whose support and hospitality is gratefully acknowledged.

APPENDIX A

Here we shall derive Eq. (3.18) from (3.17). Consider

$$Q=\mathcal{N}^{-1}\int D\mathbf{m}\,\delta(\mathrm{Tr}\mathbf{m}) \times \exp\left[-\frac{\Delta}{\sigma}\sum_i^N [\mathrm{Tr}\mathbf{m}_i^+\mathbf{m}_i + \frac{1}{d+1}\mathrm{Tr}\mathbf{m}^2]\right] \times \prod_i^N \int dp_i^2\delta[p_i^2 - p_{i-1}^+ e^{\Delta\mathbf{m}_i^+}e^{\Delta\mathbf{m}_i}p_{i-1}] \ . \quad (A1)$$

Expanding to second order in Δ, we have

$$e^{\Delta\mathbf{m}^+}e^{\Delta\mathbf{m}} = 1+2\Delta\mathbf{u}+2\Delta^2\mathbf{u}^2+\Delta^2[\mathbf{u},\omega] \ , \quad (A2)$$

where $\mathbf{m}=\mathbf{u}+\omega$ and $\mathbf{m}^+=\mathbf{u}-\omega$. Introducing $\tilde{\sigma}\equiv\sigma(d+1)/(d+2)$,

$$Q=\mathcal{N}^{-1}\int D\mathbf{u}\,\delta(\mathrm{Tr}\mathbf{u})\int D\omega\int Dp\,\exp\left[-\frac{\Delta}{\tilde{\sigma}}\sum_i \mathrm{Tr}(\mathbf{u}_i^2+\frac{d}{d+2}\omega_i^+\omega_i)\right] \times \exp\left[i\sum_i k_i[p_i^2-p_{i-1}^2-2\Delta\,\mathrm{Tr}(\mathbf{u}_i p_{i-1}p_{i-1}^+)-2\Delta^2\,\mathrm{Tr}(\mathbf{u}_i^2 p_{i-1}p_{i-1}^+)-\Delta^2\,\mathrm{Tr}([\mathbf{u},\omega]p_{i-1}p_{i-1}^+)]\right]$$
$$\approx \int D\mathbf{u}\int Dk\int Dp^2\exp\left\{-\frac{\Delta}{\tilde{\sigma}}\sum_i\left[1+i\frac{2\Delta\tilde{\sigma}}{d}p_{i-1}^2k_i\right]\mathrm{Tr}\mathbf{u}_i^2+i\sum_i k_i[p_i^2-p_{i-1}^2-2\Delta\,\mathrm{Tr}(\mathbf{u}_i p_{i-1}p_{i-1}^+)]\right\} \times \int D\zeta\exp\left[i\sum_j\zeta_j\,\mathrm{Tr}\mathbf{u}_j\right]$$

$$\approx \int Dk \int Dp^2 \prod_i \left[1+i\Delta\frac{2\tilde{\sigma}}{d}p_{i-1}^2 k_i \right]^{-[d(d+1)-2]/4} \exp\left[-\Delta\tilde{\sigma}\frac{d-1}{d}\sum_i k_i^2(p_{i-1}^2)^2 + i\sum_i k_i(p_i^2-p_{i-1}^2) \right]$$
$$\approx \int Dp^2 \left[\prod_{i=1}^{N} \frac{1}{p_{i-1}^2} \right] \exp\left\{ -\frac{\Delta}{4\tilde{\sigma}}\frac{d}{d-1}\sum_i \left[\frac{p_i^2-p_{i-1}^2}{p_i^2\Delta} - \frac{(d+2)(d-1)}{2d}\tilde{\sigma} \right]^2 \right\}$$
$$\approx \left[\prod_{i=1}^{N} \int \frac{dp_i^2}{p_i^2} \right] \left[\frac{p^2(T)}{p^2(0)} \right] \exp\left\{ -\frac{1}{4\tilde{\sigma}}\frac{d}{d-1}\int_0^T dt \left[\partial_t \ln p^2 - \frac{(d+2)(d-1)}{2d}\tilde{\sigma} \right]^2 \right\}$$
$$\approx \int Dx \exp\left[\left[\frac{d+2}{2}+2 \right][x(T)-x(0)] \right] \exp\left[-\frac{1}{\tilde{\sigma}}\frac{d}{d-1}\int_0^T dt\, \dot{x}^2 \right] . \tag{A3}$$

The second line is obtained by integrating over the matrix vorticity field ω to leading order in Δ, and observing that of $Q(\Delta^2)$ terms, only the "diagonal" part of

$$\Delta^2 \operatorname{Tr}(\mathbf{u}_i^2 p_{i-1} p_{i-1}^+) \rightarrow \frac{\Delta^2}{d} p_{i-1}^2 \operatorname{Tr}\mathbf{u}_i^2$$

can survive the continuum limit $\Delta \rightarrow 0$, as seen in the next three lines. The 3^d line is obtained by integrating over $[d(d+1)]/2$ independent components of the strain matrix $\mathbf{u}$ with the incompressibility, $\operatorname{Tr}\mathbf{u}=0$ constraint imposed by the Lagrange multiplier ζ. In the fourth line the product is reexponentiated and integration over auxiliary k is performed. Finally, the continuum limit is taken and the $x \equiv \frac{1}{2}\ln p^2$ variable is introduced. We define the secular growth exponent $\gamma \equiv (d+6)/2d$ and choose units such that $\tilde{\sigma}(d-1)/d=2$. Equation (3.18) of the text follows.

APPENDIX B: SCALAR GREEN'S FUNCTION AND LOGNORMALITY

In this appendix we compare various approximations for the path-integral expression:

$$Q(\lambda,T) = \int Dx\, e^{-\frac{1}{2}\int_0^T (\dot{x}-\gamma)^2} e^{-(\lambda^2/2)\int_0^T e^{2x}} , \tag{B1}$$

where $T>0$, $x(0)=0$, and $x(T)$ is integrated over. The normalization $Q(0)=1$ is satisfied since γ may be shifted away via $x \rightarrow \gamma t + y$, and the usual diffusion Green's-function integrates to 1. As before, rewrite

$$Q(\lambda) = e^{-\frac{1}{2}\gamma^2 T}\int_{-\infty}^{\infty} dx\, e^{\gamma x} \mathscr{g}(x,T) , \tag{B2}$$

where

$$\left[\partial_t - \tfrac{1}{2}\partial_x^2 + \frac{\lambda^2}{2}e^{2x} \right] \mathscr{g}(x,t) = \delta(x)\delta(t) . \tag{B3}$$

The latter equation after a Laplace transform in time,

$$\mathscr{g}(x,s) = \int_0^\infty e^{-st}\mathscr{g}(x,t)dt ,$$

reduces to the modified Bessel's equation under the substitution $z=e^x$. Hence,

$$\mathscr{g}(x,s) = 2\Theta(x) I_{-i\nu}(\lambda) K_{-i\nu}(\lambda e^x) + 2\Theta(-x) K_{-i\nu}(\lambda) I_{-i\nu}(\lambda e^x) , \tag{B4}$$

where $\nu^2 = -2s$ and $\lambda > 0$ in order that $g \rightarrow 0$ as $x = +\infty$. The Laplace inversion is done over a contour in s from $-i\infty$ to $+i\infty$ with $\operatorname{Re}s > 0$ which since K and I are entire in ν may be deformed into a ν contour running from $+\infty$ to $-\infty$ with $\operatorname{Im}\nu > 0$. The choice of root in the index of I and K permits us to write

$$\lim_{\lambda \rightarrow 0} I_{-i\nu}(\lambda) K_{-i\nu}(\lambda e^x) = \frac{i e^{i\nu x}}{2\nu}$$

and, hence,

$$\mathscr{g}(x,T) = \int_{i\varepsilon-\infty}^{i\varepsilon+\infty} \frac{\nu\, d\nu}{2\pi i} e^{-(\nu^2/2)T} \tilde{\mathscr{g}}(x,\nu) \tag{B5a}$$

$$\underset{\lambda\rightarrow 0}{=} \int_{i\varepsilon-\infty}^{i\varepsilon+\infty} \frac{d\nu}{2\pi} e^{i\nu|x|} e^{-(\nu^2/2)T} . \tag{B5b}$$

The latter formula is the correct free particle $\mathscr{g}$.

The integral over x in (B2) is most easily performed by interchanging it with the ν integral in (B5a) and evaluating it with the aid of the formula

$$\int_0^\infty z^{\gamma-1} K_{-i\nu}(z) dz = 2^{\gamma-2} \left| \Gamma\left[\frac{\gamma+i\nu}{2} \right] \right|^2$$

valid for $\operatorname{Re}(\gamma+i\nu)>0$. (It is at this step that we lose contact with the free-particle limit.) The remaining pieces of the x integral cancel if one uses the expression relating $K_{-i\nu}$ to $I_{\pm i\nu}$, sets $\varepsilon=0$ in (B5a), and uses the $\nu \rightarrow -\nu$ symmetry. Finally,

$$Q(\lambda) = e^{-\frac{1}{2}\gamma^2 T}\int_{\infty}^{\infty} \frac{\nu\, d\nu}{4\pi i} e^{-(\nu^2/2)T} I_{-i\nu}(\lambda) \left[\frac{2}{\lambda} \right]^\gamma \times \left| \Gamma\left[\frac{\gamma+i\nu}{2} \right] \right|^2 . \tag{B6}$$

Note the singularity at $\lambda=0$, which could have been inferred from (B2) by eliminating λ from the potential in (B3) by setting $x = x - \ln\lambda$. Evidently the concomitant change in the $x(0)$ boundary condition is immaterial.

The large-T limit of (B6) is most readily evaluated by using the symmetry $\nu \rightarrow -\nu$ to replace $I_{-i\nu}$ by $i\pi^{-1}\sinh(\pi\nu) K_{i\nu}$. Then,

$$\lim_{T\to\infty} Q(\lambda)=\frac{e^{-(\gamma^2/2)T}}{T^{3/2}}K_0(\lambda)\left[\frac{2}{\lambda}\right]^{\gamma}\frac{\Gamma^2(\gamma/2)}{2\sqrt{2\pi}}\times[1+O(T^{-1})]\ . \tag{B7}$$

For small λ, $K_0 \sim -\frac{1}{2}\ln\lambda$.

It is interesting to compare (B7) with the dissipation in (B1) replaced by its local limit, viz.,

$$Q_{\text{local}}(\lambda)=\int_{-\infty}^{\infty}\frac{dx}{\sqrt{2\pi T}}\exp\left[-\frac{\lambda^2}{2}e^{2x}-\frac{(x-\gamma T)^2}{2T}\right]=\frac{e^{-(\gamma^2/2)T}}{2\sqrt{2\pi T}}(2\lambda^{-2})^{\gamma/2}\Gamma(\gamma/2)[1+Q(1/T)]\ , \tag{B8}$$

where Q is again normalized to $Q(0)=1$. Hence, if (B8) were used in (32), there would be a change in the prefactor but not in the essential conclusion that $G(q,T)$ behaves as a step function.

Equation (B1) can be interpreted as the characteristic function of $\int_0^T dt\,\omega(t)e^x$, where $\omega(t)$ is white noise so there should be some similarity between (B6) and the generating function for the log-normal distribution. Take T pure imaginary, and wrap the ν contour around the positive imaginary axis so it runs from $i\infty$ to zero with $\text{Re}\nu<0$ and from zero back to $i\infty$ with $\text{Re}\nu>0$. For convergence it is essential that $I_{-i\nu}$ and not $K_{i\nu}$ is used in (B6). The integral is then evaluated by residues to yield

$$Q(\lambda)=e^{-(\gamma^2/2)T}\sum_{n=0}\frac{(-1)^n}{n!}(\gamma+2n)\left[\frac{2}{\lambda}\right]^{\gamma}\times I_{\gamma+2n}(\lambda)\Gamma(\gamma+n)e^{(\gamma+2n)^2T/2}\ . \tag{B9}$$

Note that each term in (B9) is analytic as $\lambda\to 0$, but that the series is divergent for $\text{Re}T>0$. In fact, (B9) could have been derived directly by iterating (B3) in powers of λ after Fourier-transforming in x, i.e.,

$$\left[\partial_t+\frac{q^2}{2}\right]\hat{\mathcal{G}}(q,t)=\delta(t)-\frac{\lambda^2}{2}\hat{\mathcal{G}}(q+2i,t)\ , \tag{B10}$$

where $\hat{\mathcal{G}}=\int_{-\infty}^{\infty}e^{-iqx}\mathcal{G}\,dx$ and (B2) is recovered by letting $q\to i\gamma$.

Let y be a log-normal variable with distribution

$$P(y)=\frac{1}{2\sqrt{2b\pi}}\frac{1}{|y|}e^{-(\ln|y|-a)^2/2b}$$

and compare the series of $R(\lambda)=\langle e^{i\lambda y}\rangle$ with (B9). For large T, to exponential accuracy, it suffices to retain only the small-λ limit of $I_{\gamma+2n}$. Therefore, comparing y^{2n} with the coefficient of $(-1)^n\lambda^{2n}/(2n)!$ in (B9), one obtains

$$\exp[(a+2nb)^2/(2b)]\cong 2^{\gamma}\frac{\Gamma(\gamma+n)}{n!}\frac{(2n)!}{\Gamma(\gamma+2n)}\times\exp[(\gamma T-\ln 2+2nT)^2/2T]\exp\left[-\frac{\ln^2 2}{2T}\right]\ , \tag{B11}$$

which quantifies the extent to which (B9) is lognormal.

APPENDIX C

Here we solve for the Green's function appearing in Eq. (4.8) which satisfies

$$\left[\partial_t-\tfrac{1}{2}\partial_x^2+\frac{\lambda^2}{2}V(x)\right]\mathcal{G}(x,t)=\delta(t)\delta(x)\ , \tag{C1}$$

with $V(x)=e^{-2\kappa e^{2x}}$ which can be approximated by a step $V(x)\approx\Theta(x_*-x)$ with $x_*=\frac{1}{2}\ln(2\kappa)\gg 1$ (for $\kappa\ll 1$). The solution for the Laplace transform of $\mathcal{G}(x,t)$ is

$$\mathcal{G}\left[x,\frac{\nu^2}{2}\right]=\frac{\theta(-x)}{2\sqrt{\nu^2+\lambda^2}}\left[1+e^{-2\sqrt{\nu^2+\lambda^2}x_*}\frac{\sqrt{\nu^2+\lambda^2}-\nu}{\sqrt{\nu^2+\lambda^2}+\nu}\right]e^{\sqrt{\nu^2+\lambda^2}x}+\frac{\theta(x)\theta(x_*-x)}{2\sqrt{\nu^2+\lambda^2}}\left[\frac{\sqrt{\nu^2+\lambda^2}-\nu}{\sqrt{\nu^2+\lambda^2}+\nu}e^{\sqrt{\nu^2+\lambda^2}(x-2x_*)}+e^{-\sqrt{\nu^2+\lambda^2}x}\right]+\frac{\theta(x-x_*)e^{-\sqrt{\nu^2+\lambda^2}x_*}}{\sqrt{\nu^2+\lambda^2}+\nu}e^{-\nu(x-x_*)}\ , \tag{C2}$$

leading to

$$\hat{P}(\lambda)=e^{-(\gamma^2/2)T}\int_{\Gamma}\frac{d\nu^2}{2\pi i}e^{(\nu^2/2)T}\left[\frac{e^{(\gamma-\sqrt{\nu^2+\lambda^2})x_*}}{\nu+\sqrt{\nu^2+\lambda^2}}\left[\frac{1}{\nu-\gamma}+\frac{\nu+\gamma}{\gamma^2-\nu^2-\lambda^2}\right]-\frac{1}{\gamma^2-\nu^2-\lambda^2}\right]\ . \tag{C3}$$

Note the normalization condition $\hat{P}(0)=1$ is satisfied by the last term. For $\text{Re}\nu>0$ and $\text{Im}\lambda=0$ the integrand of (C3) is analytic except for a pole at $\nu=\gamma$, so that

$$\hat{P}(\lambda)=\frac{2\gamma e^{(\gamma-\sqrt{\gamma^2+\lambda^2})x_*}}{\gamma+\sqrt{\gamma^2+\lambda^2}}+e^{-(\gamma^2/2)T}\int_{-\infty+i\varepsilon}^{\infty+i\varepsilon}\frac{\nu^2 d\nu}{2\pi\gamma^2}\frac{e^{-(\nu^2/2)T}e^{(\gamma-\sqrt{\lambda^2-\nu^2})x_*}}{\gamma+\sqrt{\lambda^2-\nu^2}}\ . \tag{C4}$$

In the large-T limit, the dominant contribution is the one from the pole leading to

$$\hat{P}(\lambda)=\frac{2\gamma e^{(\gamma-\sqrt{\gamma^2+\lambda^2})x_*}}{\gamma+\sqrt{\gamma^2+\lambda^2}}+O(T^{-3/2}e^{-(\gamma^2/2)T}) . \qquad (C5)$$

The first term in (C4) has a strip of analyticity in the complex λ plane of width γ, and satisfies $\hat{P}(0)=1$. The second term in (C4) has a branch cut extending down to the real axis, but its contribution to $P(\theta)$ is small because of the $\exp(-\gamma^2T/2)$ prefactor.

APPENDIX D

The study of the gradient PDF calls for the evaluation of the generating function

$$\hat{P}(\vec{\lambda},T)=\int Dx \exp\left[-\tfrac{1}{2}\int_T^0 dt\,(\dot{x}-\gamma)^2\right] \times \exp\left[-\frac{\lambda^2}{2}\int_T^0 dt\, e^{2x}e^{-\kappa e^2}\right] =e^{-(\gamma^2/2)T}\int dx\, e^{\gamma x}\tilde{\mathscr{g}}(x,T) , \qquad (D1)$$

with the Green's function $\tilde{\mathscr{g}}(x,T)$ solving

$$\left[\partial_t-\tfrac{1}{2}\partial_x^2+\frac{\lambda^2}{2}V(x)\right]\tilde{\mathscr{g}}(x,t)=\delta(t)\delta(x) , \qquad (D2)$$

with the effective potential

$$V(x)\equiv e^{2x}e^{-\kappa e^{2x}}\approx e^{2x}\Theta(x_*-x) , \qquad (D3)$$

where, as before, we will approximate the double exponential by the $x_*\approx\frac{1}{2}\ln\kappa^{-1}$ cutoff.

In contrast to (3.19), we now have to consider three regions: (1) $x<0$, (2) $0<x<x_*$, and (3) $x>x_*$, and match by requiring continuity of $\tilde{\mathscr{g}}(x,t)$ and $\partial_x\tilde{\mathscr{g}}(x,t)$, except for

$$\partial_x\tilde{\mathscr{g}}(0^+,t)-\partial_x\tilde{\mathscr{g}}(0^-,t)=1$$

as required for the Green's function. Taking the Laplace transform with respect to "t" and denoting $s=\frac{1}{2}\nu^2$, the Laplace variable we have for $x<0$ is

$$\tilde{\mathscr{g}}\left[x,\frac{\nu^2}{2}\right]=I_\nu(\lambda e^x)\left[I_\nu(\lambda)\frac{K_{\nu-1}(\lambda^{x_*})}{I_{\nu-1}(\lambda e^{x_*})}+K_\nu(\lambda)\right] ; \qquad (D4a)$$

for $0<x<x_*$,

$$\tilde{\mathscr{g}}\left[x,\frac{\nu^2}{2}\right]=I_\nu(\lambda)\left[I_\nu(\lambda e^x)\frac{K_{\nu-1}(\lambda e^{x_*})}{I_{\nu-1}(\lambda e^{x_*})}+K_\nu(\lambda e^x)\right] ; \qquad (D4b)$$

and for $x>x_*$,

$$\tilde{\mathscr{g}}\left[x,\frac{\nu^2}{2}\right]=\frac{I_\nu(\lambda)e^{-\nu(x-x_*)}}{I_{\nu-1}(\lambda e^{x_*})} .$$

Inverting the Laplace transform and substituting back into (D1),

$$\begin{aligned}\hat{P}(\lambda,T)=&\,e^{-(\gamma^2/2)T}e^{\gamma x_*}\int_0^\infty dx\, e^{\gamma x}\int_\Gamma\frac{d\nu^2}{2\pi i}e^{(\nu^2/2)T}\frac{I_\nu(\lambda)e^{-\nu x}}{\lambda e^{x_*}I_{\nu-1}(\lambda e^{x_*})}\\ &+e^{-(\gamma^2/2)T}\int_0^{x_*}dx\, e^{\gamma x}\int_\Gamma\frac{d\nu^2}{2\pi i}e^{(\nu^2/2)T}I_\nu(\lambda)\left[I_\nu(\lambda e^x)\frac{K_{\nu-1}(\lambda e^{x_*})}{I_{\nu-1}(\lambda e^{x_*})}+K_\nu(\lambda e^x)\right]\\ &+e^{-(\gamma^2/2)T}dx\, e^{\gamma x}\int_\Gamma\frac{dv^2}{2\pi i}e^{(\nu^2/2)T}I_\nu(\lambda e^x)\left[I_\nu(\lambda)\frac{K_{\nu-1}(\lambda e^{x_*})}{I_{\nu-1}(\lambda e^{x_*})}+K_\nu(\lambda)\right] .\end{aligned} \qquad (D5)$$

Note that the analytic continuation formulas

$$I_\nu(-z)=e^{i\pi\nu}I_\nu(z) \qquad (D6a)$$

and

$$K_\nu(-z)=e^{-i\pi\nu}[K_\nu(z)-i\pi I_\nu(z)] \qquad (D6b)$$

provide expression (D4) with invariance under $\lambda\to-\lambda$. Observing that I_ν and K_ν are analytic functions of ν in the $\mathrm{Re}\nu>0$ domain and $I_\nu(z)\neq0$ for any real z, we perform the x integration followed by the ν contour integral in the first term. The latter has contribution from the $\nu=\gamma$ pole and the imaginary ν axis. In the remaining terms, the ν contour is deformed to the imaginary axis and the terms are recombined using the $\nu\to-\nu$ symmetry and Bessel functions:

$$\hat{P}(\lambda)=\frac{\lambda^{-\gamma}I_\gamma(\lambda)}{(\lambda e^{x_*})^{-\gamma+1}I_{\gamma-1}(\lambda e^{x_*})}+e^{-(\gamma^2/2)T}e^{\gamma x_*}\int_{-\infty}^{\infty}\frac{\nu\,d\nu}{\pi i}e^{-(\nu^2/2)T}\frac{I_{i\nu}(\lambda)}{\lambda e^{x_*}I_{i\nu-1}(\lambda e^{x_*})}\frac{1}{i\nu-\gamma}$$
$$+e^{-(\gamma^2/2)T}\int_{-\infty}^{\infty}\frac{\nu\,d\nu}{\pi i}e^{-(\nu^2/2)T}\left\{I_{i\nu}(\lambda)\frac{K_{i\nu-1}(\lambda e^{x_*})}{I_{i\nu-1}(\lambda e^{x_*})}\int_0^{e^{x_*}}dz\,z^{\gamma-1}I_{i\nu}(\lambda z)-\frac{i}{\pi}\sinh(\pi\nu)K_{i\nu}(\lambda)\int_0^{e^{x_*}}dz\,z^{\gamma-1}K_{i\nu}(\lambda z)\right\}. \tag{D7}$$

For large T, the ν integrals are dominated by the $\nu=0$ saddle point and we find

$$\hat{P}(\lambda)=\frac{\lambda^{-\gamma}I_\gamma(\lambda)}{(\lambda e^{x_*})^{-\gamma+1}I_{\gamma-1}(\lambda e^{x_*})}-\left[\frac{2}{\pi}\right]^{1/2}T^{-3/2}\gamma^{-2}e^{-(\gamma^2/2)T}e^{\gamma x_*}\frac{I_0(\lambda)}{\lambda e^{x_*}I_1(\lambda e^{x_*})}$$
$$-\left[\frac{2}{\pi}\right]^{1/2}T^{-3/2}e^{-(\gamma^2/2)T}K_0(\lambda)\frac{K_1(\lambda e^{x_*})}{I_1(\lambda e^{x_*})}\int_0^{e^{x_*}}dz\,z^{\gamma-1}I_0(\lambda z)$$
$$-\left[\frac{2}{\pi}\right]^{1/2}T^{-3/2}e^{-(\gamma^2/2)T}\left[K_0(\lambda)+I_0(\lambda)\frac{K_1(\lambda e^{x_*})}{I_1(\lambda e^{x_*})}\right]\int_0^{e^{x_*}}dz\,z^{\gamma-1}K_0(\lambda z)\,. \tag{D8}$$

The integral in the 3^d term is bounded by $e^{\gamma x_*}K_0(\lambda)I_0(\lambda e^{x_*})$ which makes it (for $\lambda e^{x_*}\gg 1$) of the same order as the second term. The upper limit of the integral in the last term can be sent to infinity (under the same condition) which reduces it to the form of (B2) or (B6).

---

[1] C. van Atta and J. Park, in *Statistical Models and Turbulence,* edited by M. Rosenblatt and C. van Atta (Springer, Berlin, 1972), p. 402.
[2] F. Anselmet, Y. Gagne, E. Hopfinger, and R. Antonia, J. Fluid Mech. **140**, 63 (1984).
[3] B. Castaing, Y. Gagne, and E. J. Hopfinger, Physica D **46**, 177 (1990).
[4] B. Castaing *et al.*, J. Fluid Mech. **204**, 1 (1989).
[5] J. P. Gollub *et al.*, Phys. Rev. Lett. **67**, 3507 (1991); B. R. Lane *et al.*, Phys. Fluids A **5**, 2255 (1993).
[6] Jayesh and Z. Warhaft, Phys. Rev. Lett. **67**, 3503 (1991); Phys. Fluids A **4**, 2307 (1992).
[7] S. T. Thoroddsen and C. van Atta, J. Fluid Mech. **44**, 547 (1992). These authors did not find any exponential tails of the PDF when the temperature gradient was strong enough to make the flow significantly stably stratified. The tails of the distribution are more sensitive to the stratification since, as we will show, they correspond to temperature transported from several integral scales away.
[8] G. E. Batchelor, J. Fluid Mech. **5**, 113 (1959).
[9] R. H. Kraichnan, Phys. Fluids **11**, 945 (1968).
[10] R. H. Kraichnan, J. Fluids Mech. **64**, 737 (1974).
[11] M. B. Isichenko, Rev. Mod. Phys. **64**, 961 (1992). The path-integral derivation of the Taylor diffusion formula appears in I. T. Drummond, J. Fluid Mech. **123**, 59 (1982).
[12] P. B. Rhines and W. R. Young, J. Fluid Mech. **133**, 133 (1983).
[13] E. Ott and T. M. Antonsen, Phys. Rev. A **39**, 3660 (1989).
[14] A. J. Majda, Phys. Fluids A **5**, 1963 (1993).
[15] A. Pumir, B. Shraiman, and E. Siggia, Phys. Rev. Lett. **66**, 2984 (1991).
[16] M. Holzer and A. Pumir, Phys. Rev. E **47**, 2020 (1993).
[17] This point of view was first advanced by R. Kraichnan and Y. Kimura, Phys. Fluids A **5**, 2264 (1993).
[18] In this sense the situation is analogous to the solid-state physics problem of Lifshitz tails of the density of states for a random potential [see Itzykson and Drouffe, *Statistical Field Theory* (Cambridge University, Cambridge, England, 1989], where the probability of a low-energy state is determined by the probability of a large fluctuation of the potential in an extended region.
[19] C. Gibson, C. Freihe, and S. McConnell, Phys. Fluids **20**, 5156 (1977).
[20] Simulations have been performed by M. Holzer and E. Siggia (unpublished) and A. Pumir (private communication).
[21] J. P. Eckmann and D. Ruelle, Rev. Mod. Phys. **57**, 617 (1985).
[22] The white-noise limit here is not essential and the limit $t\gg\tau$ would suffice. The special configuration of strain with the principal axis of $\mathbf{M}^+(t',t)\mathbf{M}(t',t)$ aligned for different times to better than $e^{-\gamma|t-t'|}$ would retain the **Q** dependence of the RHS of (4.4) and allow the latter to be made small for q within $e^{-\gamma|t|}$ of some fixed direction. These constraints, however, make the contribution to the ensemble average negligible.
[23] A. Kerstein, J. Fluid Mech. **231**, 361 (1991).
[24] A. S. Monin and A. M. Yaglom, *Statistical Fluid Dynamics* (MIT, Cambridge, MA, 1975).
[25] R. Kraichnan, Phys. Fluids **8**, 575 (1968).
[26] A. Polyakov (unpublished).